



## Control of Optical Transitions with Magnetic Fields in Weakly Bound Molecules

B. H. McGuyer,<sup>1</sup> M. McDonald,<sup>1</sup> G. Z. Iwata,<sup>1</sup> W. Skomorowski,<sup>2,\*</sup> R. Moszynski,<sup>2</sup> and T. Zelevinsky<sup>1,†</sup>

<sup>1</sup>Department of Physics, Columbia University, 538 West 120th Street, New York, New York 10027-5255, USA

<sup>2</sup>Department of Chemistry, Quantum Chemistry Laboratory, University of Warsaw, Pasteura 1, 02-093 Warsaw, Poland

(Received 20 March 2015; published 28 July 2015)

In weakly bound diatomic molecules, energy levels are closely spaced and thus more susceptible to mixing by magnetic fields than in the constituent atoms. We use this effect to control the strengths of forbidden optical transitions in  $^{88}\text{Sr}_2$  over 5 orders of magnitude with modest fields by taking advantage of the intercombination-line threshold. The physics behind this remarkable tunability is accurately explained with both a simple model and quantum chemistry calculations, and suggests new possibilities for molecular clocks. We show how mixed quantization in an optical lattice can simplify molecular spectroscopy. Furthermore, our observation of formerly inaccessible  $f$ -parity excited states offers an avenue for improving theoretical models of divalent-atom dimers.

DOI: 10.1103/PhysRevLett.115.053001

PACS numbers: 33.80.-b, 31.15.A-, 33.20.-t, 33.70.Fd

Transitions between quantum states are the basis for spectroscopy and the heart of atomic clocks. The ability to access a transition experimentally depends on the transition mechanism and the states involved. For atoms and molecules, the dominant mechanism is the electric-dipole interaction, and electric-dipole transitions are only allowed between angular-momentum eigenstates with opposing parity that satisfy the rigorous selection rules  $\Delta J \equiv J' - J = 0, \pm 1$  and  $\Delta m \equiv m' - m = 0, \pm 1$  (but  $\Delta J \neq 0$  if  $J = 0$ ), where  $J$  and  $m$  are the total and projected angular momentum quantum numbers, and primes refer to the higher-energy states. Accessible transitions that are forbidden by these rules or the additional rules that arise, for example, from molecular symmetries, are of great interest because they are associated with long-lived quantum states and enable precision measurements such as parity-violation experiments [1–4]. Forbidden transitions are central to atomic time keeping and have been extensively researched in order to advance the state of the art [5,6].

In this Letter, we demonstrate how the control of forbidden transitions with applied magnetic fields is greatly enhanced by the dense level structure of molecules as compared to atoms. We use modest fields of a few tens of gauss to not only enable strongly forbidden transitions, but yield transition strengths comparable to allowed transitions. In contrast, several million gauss would be needed to achieve the same results using the atoms that form these molecules. The physics that enables this tuning of transition strengths by 5 orders of magnitude also leads to highly nonlinear Zeeman shifts which we precisely measure. We explain our observations with an intuitive as well as a rigorous theoretical model, and suggest how they may be used to improve such models and to engineer an optical molecular clock.

Figure 1 illustrates the process of magnetically enabling a forbidden transition in  $^{88}\text{Sr}_2$  molecules near the atomic

$^1S_0 - ^3P_1$  intercombination line. While the physics responsible for the effect is not unique to  $^{88}\text{Sr}_2$ , this narrow ( $\sim 10$  kHz) optical transition allows us to (i) spectroscopically address very weakly bound molecules where the energy level density and the magnetic moment are large, and (ii) trap and probe the molecules in an optical lattice without spectral broadening and thus attain sensitivity to

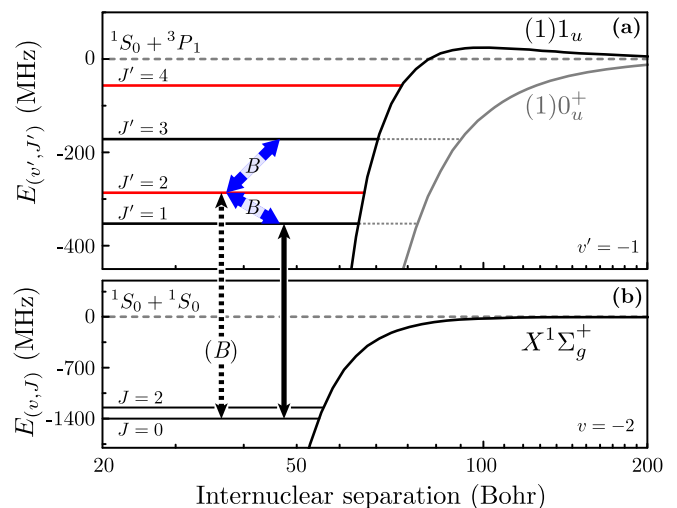


FIG. 1 (color online). A magnetically enabled forbidden molecular transition. (a) Admixing of excited states by an applied static magnetic field  $B$  (slanted arrows). Near the  $^1S_0 + ^3P_1$  asymptote, two molecular potentials,  $1_u$  and  $0_u^+$ , are optically accessible from the ground state,  $X^1\Sigma_g^+$ . States with odd  $J'$  are of both  $1_u$  and  $0_u^+$  character because of nonadiabatic Coriolis coupling [7]. This coupling is not essential to this work, and only admixing of  $1_u$  states is shown for clarity. (b) An optical transition from  $J = 0$  to  $J' = 2$  is forbidden (dashed vertical arrow), while to  $J' = 1$  is allowed (solid vertical arrow). With an applied field, the forbidden transition becomes allowed because of admixing with the  $J' = 1$  state.

tiny transition strengths. Starting from a ground state with  $J = 0$ , a transition to an excited state with  $J' = 1$  is allowed (solid arrow in Fig. 1). A transition to  $J' = 2$ , in contrast, is forbidden (dashed arrow). However, applying a static magnetic field couples the excited states (blue arrows), making the energy eigenstates no longer angular-momentum eigenstates. Thus, the excited state originally described by  $J' = 2$  acquires a  $J' = 1$  component that now satisfies the selection rules for a transition from  $J = 0$ . In this way, applying a magnetic field enables the forbidden transition with  $\Delta J = 2$ .

We measured this variation of transition strengths with an applied magnetic field  $B$  for ultracold  $^{88}\text{Sr}_2$  in an optical lattice. The experimental apparatus follows Refs. [7,8]. The results are arranged by increasing  $|\Delta J|$  in Fig. 2. As shown, moderate magnetic fields are able to strongly control the strength of transitions between ground- and excited-state molecules near the intercombination line. We are able to drive forbidden transitions with  $|\Delta J|$  up to 3 and to control transition strengths over 5 orders of magnitude to nearly reach the allowed transition strengths.

Our data are supported by the theoretical calculations shown in Fig. 2 (curves). Qualitatively, we explain these observations as follows. Consider a transition between a ground state  $|\gamma\rangle$  and an excited state  $|\mu\rangle$ . The strength of this transition is proportional to the square  $|\Omega_{\gamma\mu}|^2$  of the Rabi frequency  $\Omega_{\gamma\mu} = \langle\gamma|H_e|\mu\rangle/\hbar$ , where  $H_e$  is the electric-dipole interaction Hamiltonian and  $\hbar$  is the reduced Planck constant. Applying a static magnetic field perturbs the states and thus the strength of the transition. To first order in the field strength  $B$ , the excited state becomes

$$|\mu(B)\rangle \approx |\mu(0)\rangle + \sum_{\nu \neq \mu} (B/B_{\mu\nu})|\nu(0)\rangle, \quad (1)$$

where the characteristic magnetic fields  $B_{\mu\nu} = (E_\mu - E_\nu)/\langle\mu(0)|H_Z/B|\nu(0)\rangle$  give the admixing per unit  $B$  for the pairs of states with energies  $E_\mu$  and  $E_\nu$ , and the sum is over all states that couple to  $|\mu\rangle$  via the Zeeman interaction  $H_Z = \mu_B(g_L\mathbf{L} + g_S\mathbf{S}) \cdot \mathbf{B}$  [7]. The field  $\mathbf{B} = B\hat{z}$  defines our quantization axis, and  $H_Z$  couples states with  $\Delta m = 0$  and  $\Delta J = 0, \pm 1$  (but  $\Delta J \neq 0$  if  $J = 0$ ). We assume  $|\gamma(B)\rangle \approx |\gamma(0)\rangle$  because spinless  $^{88}\text{Sr}_2$  molecules in the electronic ground state interact very weakly with the magnetic field.

As a result, the strength of the transition changes with the applied field as

$$|\Omega_{\gamma\mu}(B)|^2 \approx |\Omega_{\gamma\mu}(0)|^2 + B^2 \left| \sum_{\nu \neq \mu} \frac{\Omega_{\gamma\nu}(0)}{B_{\mu\nu}} \right|^2 + B \sum_{\nu \neq \mu} \left( \frac{\Omega_{\gamma\mu}(0)\Omega_{\gamma\nu}^*(0)}{B_{\mu\nu}^*} + \frac{\Omega_{\gamma\mu}^*(0)\Omega_{\gamma\nu}(0)}{B_{\mu\nu}} \right). \quad (2)$$

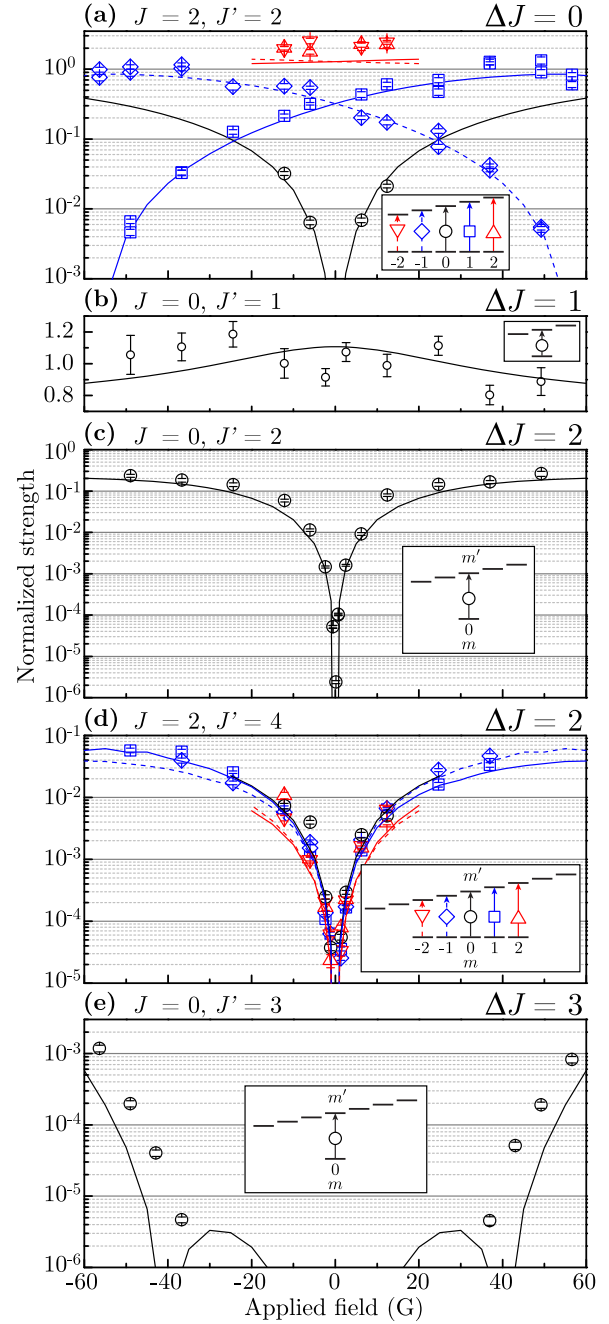


FIG. 2 (color online). Magnetic control of molecular transitions in  $^{88}\text{Sr}_2$  near the intercombination line. Points are experimental values and curves are theoretical calculations. The  $\pi$  transitions are between  $X^1\Sigma_g^+(v = -2, J, m)$  ground states and  $1_u(v' = -1, J', m')$  excited states for  $J' = 1, 2, 4$ , or the  $0_u^+(v' = -3, J', m')$  excited state for  $J' = 3$  [9]. (a) An allowed transition with  $\Delta J = 0$  has an “accidentally” forbidden  $m' = 0$  component that becomes allowed with field, and  $m' = \pm 1$  components that show field-induced interference from admixing. (b) An allowed transition with  $\Delta J = 1$  is mostly field insensitive. Its average value is used to normalize the data. (c),(d) Forbidden transitions with  $\Delta J = 2$  and strengths that vary over 5 orders of magnitude to become comparable to allowed transitions. (e) A highly forbidden transition with  $\Delta J = 3$  enabled by second-order admixing.

For a forbidden transition, the first and last terms are zero, so the strength will be quadratic in  $B$  if  $|\mu\rangle$  admixes with a state  $|\nu\rangle$  for which the transition would be allowed. This is what we observe at low fields in Figs. 2(c) and 2(d) and, additionally, in Fig. 2(a) for the “accidentally” forbidden  $m = m' = 0$  component of an allowed transition [10]. For allowed transitions, all the terms in Eq. (2) may contribute. The first term is field insensitive and dominates in Fig. 2(b). The third term is linear with  $B$  and represents the destructive or constructive interference that we observe with  $m = m' = \pm 1$  components in Fig. 2(a). Finally, the behavior of the highly forbidden transition in Fig. 2(e) is roughly quartic with  $B$ , and comes from higher-order admixing beyond this approximate model.

Besides affecting transition strengths, the applied field produces highly nonlinear Zeeman shifts of the excited states, as shown in Fig. 3. We observe shifts up to sixth order in  $B$ , well beyond the quadratic shifts reported previously for  $^{88}\text{Sr}_2$  or similar dimers [7,11,12], and find good agreement with calculations as shown in Table I. We parametrize these shifts as the sum of linear and nonlinear terms [7]

$$\Delta E_b = g(v', J')\mu_B m' B + \sum_{n>1} q_n(v', J', m')\mu_B B^n, \quad (3)$$

where  $\mu_B$  is the Bohr magneton. Here, the binding energies  $E_b$  are negative, so positive shifts make molecules less bound. The sum extends over the fewest terms needed to summarize the data, following the symmetry  $\Delta E_b(-m', -B) = \Delta E_b(m', B)$ . We used pure  $\sigma$  transitions to measure the signs of  $g(v', J')$ .

The dense level structure of  $^{88}\text{Sr}_2$  molecules allows the observation of these effects near the intercombination line with significantly lower fields than would be needed for  $^{88}\text{Sr}$  atoms. In atoms, admixing occurs between  $^3P_{J'}$  fine structure levels with spacings  $|E_\mu - E_\nu|/h$  of several THz

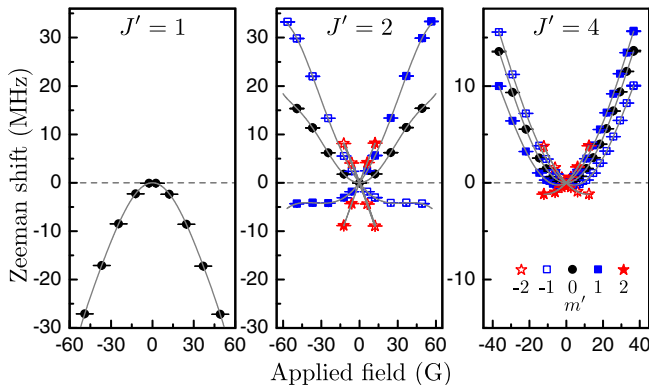


FIG. 3 (color online). Highly nonlinear Zeeman shifts for the three  $1_u(v' = -1, J')$  states listed in Table I. The  $\pi$  transitions used in the measurements are indicated in Figs. 2(b), 2(a), 2(d), respectively. The lines are polynomial fits using Eq. (3) with appropriate symmetry constraints.

[13,14]. For molecules, admixing occurs between rovibrational levels near the  $^1S_0 + ^3P_1$  threshold, with similar magnetic moments but typical spacings of several tens of MHz. As a result, the characteristic mixing fields  $|B_{\mu\nu}| \sim |E_\mu - E_\nu|/\mu_B$  are roughly several million gauss for atoms versus several tens of gauss for molecules. While these fields may be greatly reduced by choosing an atom with hyperfine structure [15] instead of  $^{88}\text{Sr}$ , the enhancement with molecules versus atoms will still be present. The enhancement would decrease, however, for more deeply bound molecules as the rovibrational spacings increase. Similar enhancement is expected with Stark-induced transitions using electric fields [16] as are often used in parity-violation experiments [1–4].

We obtained the data in Figs. 2 and 3 using procedures similar to those in Refs. [7,8]. For transition strengths, the measured quantity is  $Q \equiv A/(\tau P) = |\Omega_{\gamma\mu}(B)|^2/(4P)$  [17], where  $A$  is the Lorentzian area of the natural logarithm of an absorption dip,  $\tau$  is the probe exposure time, and  $P$  is the probe beam power. The quantity  $Q = Q(m, m')$  was measured separately for each transition component between initial  $m$  and final  $m'$  quantum numbers, and at different applied fields  $B$ , by observing the loss of ground-state molecules by absorption. The final values of  $Q$  were normalized to the average strength of the allowed transition in Fig. 2(b).

To overcome the challenges of quantum-state resolved molecular spectroscopy, we utilized a mixed quantization of the  $J = 2$  ground-state molecules from competing Zeeman shifts and tensor light shifts [17,20]. Figure 4 demonstrates this effect, showing how the depletion of a sublevel  $m$  leads to the depletion of other selected sublevels, simulating forbidden transitions with  $|\Delta m| = 2, 4$ . This effect arises because the optical lattice has an electric field  $\mathbf{E}(t) = E(t)\hat{y}$  linearly polarized orthogonally to  $\mathbf{B} = B\hat{z}$  and to the lattice axis  $\hat{x}$  (i.e., the “magic” trapping conditions for a  $^1S_0 - ^3P_1$  transition in  $^{88}\text{Sr}$  atoms [21]). The lattice light shift is therefore not diagonal along  $\mathbf{B}$ , but includes off-diagonal couplings (or “Raman coherences” [21]) between sublevels with  $|\Delta m| = 2$ . While the Zeeman shifts (3) of the excited states are large enough to suppress these couplings for typical values of  $B$ , the couplings are large enough to suppress the small Zeeman shifts of the ground states that are only on the order of a nuclear magneton [22]. As a result, the  $J = 2$  ground eigenstates are superpositions of sublevels with even or odd  $m$ , as observed in Fig. 4. To correct for these effects, the data in Fig. 2 for transitions starting from  $J = 2$  were multiplied by a correction factor  $R(m)$  after normalization, where  $R(0) = 4/3$ ,  $R(\pm 1) = 2$ , and  $R(\pm 2) = 8$ , as derived in Ref. [17]. The mixed quantization enabled our measurement protocol because it provided molecules with all  $m$  for  $J = 2$ , in particular,  $m = \pm 2$  that would be otherwise difficult to create simultaneously. Furthermore, to measure transition strengths, we only needed to count the final

TABLE I. Experimental (Expt.) and theoretical (Th.) Zeeman shifts for the  $1_u(v' = -1)$  states shown in Figs. 2 and 3. Binding energies  $E_b$  are reported to the nearest MHz. Only the parameters  $q_n = q_n(v', J', |m'|)$  ( $G^{1-n}$ ) required for a good fit with Eq. (3) are reported.

$J'$	$ E_b $		$g$		$ m' $	$q_2 \times 10^2$		$q_3 \times 10^5$		$q_4 \times 10^6$		$q_5 \times 10^9$		$q_6 \times 10^{10}$	
	(Expt.)	(Th.)	(Expt.)	(Th.)		(Expt.)	(Th.)	(Expt.)	(Th.)	(Expt.)	(Th.)	(Expt.)	(Th.)	(Expt.)	(Th.)
1	353	353	0.625(9)	0.613	0	-1.122(4)	-1.11	0	0	2.0(1)	1.85	0	0	-2.74(2)	-2.48
					1	-0.8(1)	-0.67								
2	287	288	0.2479(2)	0.250	0	0.872(6)	0.827	0	0	-2.38(6)	-2.35	0	0	2.7(1)	2.66
					1	0.599(1)	0.578	1.1(1)	1.7	-0.97(1)	-1.00	-5.6(6)	-6.06		
					2	-0.18(1)	-0.20								
4	56	61	0.0734(2)	0.075	0	0.882(1)	0.884	0	0	-1.16(1)	-1.13				
					1	0.831(1)	0.827	-2.4(1)	-2.48	-1.09(1)	-1.02	7.4(6)	7.53		
					2	0.62(1)	0.64								

population in two ground-state sublevels ( $m = 0$  and  $m = 1$  or  $-1$ ) to gather the data in Fig. 2. This was critical at large fields because of the difficulty in individually detecting  $m = \pm 2$  using the transitions available to convert molecules to atoms.

The theoretical model used the most recent electronic potentials for the  $1_u$  and  $0_u^+$  excited states of  $^{88}\text{Sr}_2$  [11], which are based on the original *ab initio* calculations [23], and the empirical potential for the ground state [24]. To reproduce the experimental observations of Zeeman shifts, nine excited-state coupled channels including  $J' = 1$  to 6

were required. Because of the sensitivity to the coupling between the channels, precise measurements of high-order Zeeman shifts as in Table I are useful to test the accuracy of theoretical models [7,11,12]. The calculated coefficients  $q_2$  and  $q_3$  are due to admixing from states with  $|\Delta J'| \leq 1$ ,  $q_4$  and  $q_5$  with  $|\Delta J'| \leq 2$ , and  $q_6$  with  $|\Delta J'| \leq 3$ . The signs of  $q_2$  for even and odd  $J'$  are typically opposite because of repulsive second-order perturbative couplings between pairs of states, which we have observed for more states than reported here (Fig. 3 and Ref. [7]).

Our direct observation of  $1_u$  levels with even values of  $J'$  suggests a way to further adjust theoretical models for homonuclear dimers of divalent atoms. These “*f*-parity” levels are inaccessible by *s*-wave photoassociation, and have not been observed previously in experiments with Sr, Yb, or Ca atoms at ultracold temperatures. In contrast, they are accessible in experiments with ultracold molecules. Rovibrational levels with even values of  $J'$  exist only for the  $1_u$  potential, so Coriolis coupling, which mixes  $1_u$  and  $0_u^+$  states for odd  $J'$ , is absent for levels with even  $J'$ . Indeed, Table I shows that the  $1_u$  levels with even  $J'$  have nearly ideal Hund’s case (c)  $g$  factors [7],  $g \approx 3/[2J'(J' + 1)]$ , while those with odd  $J'$  do not. Therefore, precise knowledge of the  $1_u$  levels with even  $J'$  will allow these potentials to be adjusted independently.

The field enabling of strongly forbidden optical transitions demonstrated here could be used to access ultranarrow molecular transitions. Particularly, magnetic tuning of transition strengths to long-lived weakly bound subradiant excited states [8] could enable subhertz optical transitions to  $0_g^+$ , possibly between a pair of spinless  $J = 0$  states [13,14]. [The  $0_g^+$  and  $1_g$  potentials are omitted from Fig. 1(a) due to their extremely weak coupling to the ground state [8].] Clocks based on molecules can complement atomic clocks, for example, via different sensitivities to fundamental constant variations [25,26].

In conclusion, we have demonstrated the remarkable control of forbidden optical transitions in weakly bound molecules by modest applied magnetic fields. Our

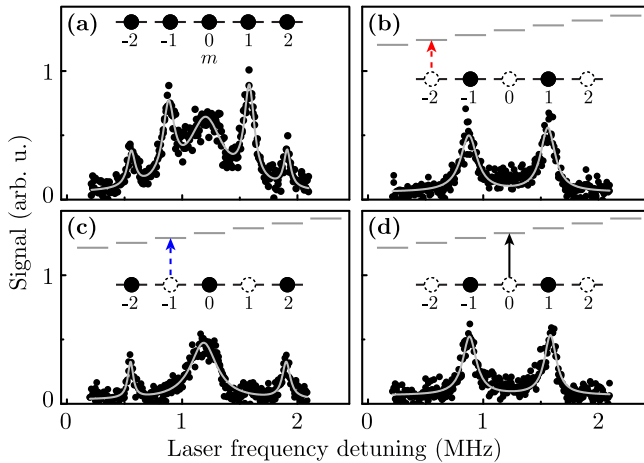


FIG. 4 (color online). Demonstration of mixed quantization of  $J = 2$  ground states by an optical lattice linearly polarized orthogonally to the applied magnetic field. (a) Spectrum measuring the populations of ground-state sublevels  $m$ . (b) A  $\pi$  transition to the  $m' = -2$  sublevel of a Zeeman-resolved excited state depletes not only the population with  $m = -2$ , but also with  $m = 0$  and  $m = 2$ . The additional population loss with  $|\Delta m| = 2, 4$  is highly forbidden by selection rules, but occurs because the optical lattice mixes the sublevels. (c) Likewise, a  $\pi$  transition to  $m' = -1$  removes the populations with  $m = \pm 1$ . (d) A  $\pi$  transition to  $m' = 0$  has the same effect as that to  $m' = -2$  shown in (b).

experiments with ultracold  $^{88}\text{Sr}_2$  molecules in an optical lattice are sensitive to exceedingly weak transitions owing to narrow intercombination lines, and demonstrate how mixed quantization can aid molecular spectroscopy as well as suggest new approaches to ultraprecise molecular clocks. The measurements of transition strengths and highly nonlinear Zeeman shifts provide a stringent test of state-of-the-art quantum chemistry calculations. The observation of  $f$ -parity excited-state molecules, in particular, opens new avenues for improvement of future theoretical models for divalent-atom dimers.

We acknowledge NIST Grant No. 60NANB13D163, ARO Grant No. W911NF-09-1-0504, ONR Grant No. N00014-14-1-0802, and NSF Grants No. DGE-2069240 and No. PHY-1349725 for partial support of this work. R. M. acknowledges the Foundation for Polish Science for support through the MISTRZ program.

\*Present address: Theoretische Physik, Universität Kassel, Heinrich Plett Straße 40, 34132 Kassel, Germany.

†tz@phys.columbia.edu

- [1] J. Guéna, M. Lintz, and M.-A. Bouchiat, Atomic parity violation: Principles recent results, present motivations, *Mod. Phys. Lett. A* **20**, 375 (2005).
- [2] A. Derevianko and S. G. Porsev, Theoretical overview of atomic parity violation, *Eur. Phys. J. A* **32**, 517 (2007).
- [3] V. A. Dzuba and V. V. Flambaum, Parity violation and electric dipole moments in atoms and molecules, *Int. J. Mod. Phys. E* **21**, 1230010 (2012).
- [4] S. B. Cahn, J. Ammon, E. Kirilov, Y. V. Gurevich, D. Murphree, R. Paolino, D. A. Rahmlow, M. G. Kozlov, and D. DeMille, Zeeman-Tuned Rotational Level-Crossing Spectroscopy in a Diatomic Free Radical, *Phys. Rev. Lett.* **112**, 163002 (2014).
- [5] A. Derevianko and H. Katori, Colloquium: Physics of optical lattice clocks, *Rev. Mod. Phys.* **83**, 331 (2011).
- [6] J. Vanier and C. Audoin, *The Quantum Physics of Atomic Frequency Standards* (A. Hilger, Bristol, 1989).
- [7] B. H. McGuyer, C. B. Osborn, M. McDonald, G. Reinaudi, W. Skomorowski, R. Moszynski, and T. Zelevinsky, Non-adiabatic Effects in Ultracold Molecules via Anomalous Linear and Quadratic Zeeman Shifts, *Phys. Rev. Lett.* **111**, 243003 (2013).
- [8] B. H. McGuyer, M. McDonald, G. Z. Iwata, M. G. Tarallo, W. Skomorowski, R. Moszynski, and T. Zelevinsky, Precise study of asymptotic physics with subradiant ultracold molecules, *Nat. Phys.* **11**, 32 (2015).
- [9] In this work, negative vibrational indices count down from the threshold, e.g.,  $v = -1$  denotes the least-bound ground state.
- [10] D. A. Varshalovich, A. N. Moskalev, and V. K. Khersonskii, *Quantum Theory of Angular Momentum* (World Scientific, Singapore, 1988).
- [11] M. Borkowski, P. Morzyński, R. Ciuryło, P. S. Julienne, M. Yan, B. J. DeSalvo, and T. C. Killian, Mass scaling and nonadiabatic effects in photoassociation spectroscopy of ultracold strontium atoms, *Phys. Rev. A* **90**, 032713 (2014).
- [12] M. Kahmann, E. Tiemann, O. Appel, U. Sterr, and F. Riehle, Photoassociation spectroscopy of  $^{40}\text{Ca}$  measured with kilohertz accuracy near the  $^3P_1 + ^1S_0$  asymptote and its Zeeman effect, *Phys. Rev. A* **89**, 023413 (2014).
- [13] A. V. Taichenachev, V. I. Yudin, C. W. Oates, C. W. Hoyt, Z. W. Barber, and L. Hollberg, Magnetic Field-Induced Spectroscopy of Forbidden Optical Transitions with Application to Lattice-Based Optical Atomic Clocks, *Phys. Rev. Lett.* **96**, 083001 (2006).
- [14] Z. W. Barber, C. W. Hoyt, C. W. Oates, L. Hollberg, A. V. Taichenachev, and V. I. Yudin, Direct Excitation of the Forbidden Clock Transition in Neutral  $^{174}\text{Yb}$  Atoms Confined to an Optical Lattice, *Phys. Rev. Lett.* **96**, 083002 (2006).
- [15] W. A. Davis, H. J. Metcalf, and W. D. Phillips, Vanishing electric dipole transition moment, *Phys. Rev. A* **19**, 700 (1979).
- [16] D. Budker, D. F. Kimball, and D. P. DeMille, *Atomic Physics: An Exploration through Problems and Solutions*, 2nd ed. (Oxford University Press, New York, 2008).
- [17] See Supplemental Material at <http://link.aps.org/supplemental/10.1103/PhysRevLett.115.053001> for a treatment of mixed quantization of molecules in an optical lattice and for descriptions of measurements and calculations of transition strengths, which includes Refs. [18,19].
- [18] A. E. Siegman, *Lasers* (University Science Books, Sausalito, CA, 1986).
- [19] G. Reinaudi, C. B. Osborn, M. McDonald, S. Kotochigova, and T. Zelevinsky, Optical Production of Stable Ultracold  $^{88}\text{Sr}_2$  Molecules, *Phys. Rev. Lett.* **109**, 115303 (2012).
- [20] M. Auzinsh, D. Budker, and S. M. Rochester, *Optically Polarized Atoms: Understanding Light-Atom Interactions* (Oxford University Press, New York, 2010).
- [21] T. Ido and H. Katori, Recoil-Free Spectroscopy of Neutral Sr Atoms in the Lamb-Dicke Regime, *Phys. Rev. Lett.* **91**, 053001 (2003).
- [22] J. M. Brown and A. Carrington, *Rotational Spectroscopy of Diatomic Molecules* (Cambridge University Press, Cambridge, England, 2003).
- [23] W. Skomorowski, F. Pawłowski, C. P. Koch, and R. Moszynski, Rovibrational dynamics of the strontium molecule in the  $A^1\Sigma_u^+$ ,  $c^3\Pi_u$ , and  $a^3\Sigma_u^+$  manifold from state-of-the-art *ab initio* calculations, *J. Chem. Phys.* **136**, 194306 (2012).
- [24] A. Stein, H. Knöckel, and E. Tiemann, The  $^1S + ^1S$  asymptote of  $\text{Sr}_2$  studied by Fourier-transform spectroscopy, *Eur. Phys. J. D* **57**, 171 (2010).
- [25] T. Zelevinsky, S. Kotochigova, and J. Ye, Precision Test of Mass-Ratio Variations with Lattice-Confined Ultracold Molecules, *Phys. Rev. Lett.* **100**, 043201 (2008).
- [26] K. Beloy, A. W. Hauser, A. Borschevsky, V. V. Flambaum, and P. Schwerdtfeger, Effect of  $\alpha$  variation on the vibrational spectrum of  $\text{Sr}_2$ , *Phys. Rev. A* **84**, 062114 (2011).